CIEMAT's outcomes from the PHEBUS-FPT1 uncertainty analysis in the framework of the EU-MUSA project

Rafael Bocanegra, Luis E. Herranz
CIEMAT
Avenida Complutense 40, 28040 Madrid, Spain
rafael.bocanegra@ciemat.es, luisen.herranz@ciemat.es

ABSTRACT

In 2019, the first European project fully focused on uncertainty quantification in severe accident analysis was launched. Referred as "Management and Uncertainties of Severe Accidents (MUSA)" and led by CIEMAT, the project foresees testing uncertainty quantification methods in a simplified but still representative scenario of a severe accident: the PHEBUS-FPT1 experiment. This study synthesizes the results got by CIEMAT when using the MELCOR 2.2 code and the DAKOTA statistical software for such a purpose. A BEPU analysis has been performed including all the input variables considered uncertain which affect the fission product release and transport phenomena. The uncertainties have been propagated applying the Monte Carlo method and the uncertainty region has been obtained according to the Wilk's method. A subsequent regression analysis, based on the Pearson's and Spearman's coefficients, has been also performed to identify the most influential parameters on the main figures of merits, being these the cesium and iodine release, and airborne mass transport to the containment. The results have indicated that the uncertainty band is broader than an order of magnitude in the case of FP transport and determined not just by particle shape but also by some thermal-hydraulic variables.

KEYWORDS

Uncertainty Quantification, Severe Accident, Source Term, PHEBUS-FPT1, MELCOR

1. INTRODUCTION

Numerical simulation tools are widely used in the nuclear community to assess the behavior of Nuclear Power Plants (NPPs) during postulated accidents, including Severe Accidents (SAs). They are a central element of the safety demonstration where the compliance of the main safety features of a NPP is assessed against safety requirements. In addition, the development and optimization of Accident Management (AM) measures, aiming at preventing and mitigating the consequences of SA, heavily rely on numerical simulations with codes such as ASTEC, AC2, MAAP, or MELCOR. Among the key parameters to predict are the time of failure of safety barriers and the potential radiological Source Term (ST) to the environment.

The EU project Management and Uncertainties Of Severe Accidents (MUSA) was founded in the HORIZON 2020 EURATOM NFRP-2018 call on "Safety assessments to improve accident management strategies for generation II and III reactors". It is coordinated by CIEMAT with the participation of 28 Organizations from 16 Countries [1]. The project aims to establish a harmonized approach for the Uncertainty Quantification (UQ) associated with Severe Accident (SA), with the main objective of assessing the capability of SA codes for estimating the uncertainty range in ST in GEN II and III Nuclear Power Plants (NPPs), as well as for Spent Fuel Pool (SFPs) accident scenarios. To do so and going beyond the State-Of-the-Art in terms of predictive capability, SA analysis codes are to be coupled with the best available or improved UQ methods and tools.

In this context, the Work Package 4 (WP4, Application of UQ Methods against Integral Experiments) is aimed at applying and testing UQ methodologies against the PHEBUS FPT1 test [2]. This paper summarizes

the CIEMAT's UQ methodology (section 2) to simulate the PHEBUS FPT1 UQ scenario (section 3). The main insights coming out from these calculations are then outlined (section 4) and finally synthesized in some final remarks and conclusions (section 5).

2. CIEMAT's UQ Methodology

The Best Estimate (BE) approach has been gaining momentum in the nuclear safety community as a means to achieve more realistic calculations than the original conservative approach applied for decades. However, a single BE calculation is not enough when safety is concerned; it needs to be complemented by assessing the precision of the calculation through considering the scattering effect on estimates caused by input and code uncertainties; CIEMAT's approach to do so is based on the BEPU-CSA methodology [3] which relies on the input-driven uncertainty propagation. Calculations are performed with the MELCOR 2.2 code [4] for the Severe Accident (SA) phenomenology complemented with the DAKOTA tool [5] for the statistical analysis. The goal of the statistical analysis is the estimation of the tolerance interval of the selected FOMs, which is achieved by means of the Wilks' order statistic method [6]. In addition, a regression analysis is also performed in order to highlight the input uncertainties influence, being this focused on Pearson's and Spearman's Correlation Coefficients (CCs).

MELCOR is a fully integrated, engineering-level computer code that models the progression of severe accidents [4]. It includes a broad spectrum of phenomena, from core degradation to source term to the environment; just to mention a few: thermal-hydraulic response in the reactor coolant system, reactor cavity, containment, and confinement buildings; core heat-up, degradation, and relocation; core-concrete attack; hydrogen production, transport and combustion; fission product release, transport and behavior.

The statistical tool DAKOTA [5] was originally conceived to more readily interface simulation codes and optimization algorithms. However, latest versions include other iterative analysis methods such as UQ. Dakota is able to perform forward uncertainty propagation in which probability information for input parameters is mapped to probability information for output response functions. CIEMAT used the DAKOTA tool in "stand-alone" mode, which required developing several python scripts to compute the Monte Carlo (MC) sequence and perform the pairing process of input parameters. The whole process is governed by another python script; whose task is just to follow the flow chart shown in Figure 1.

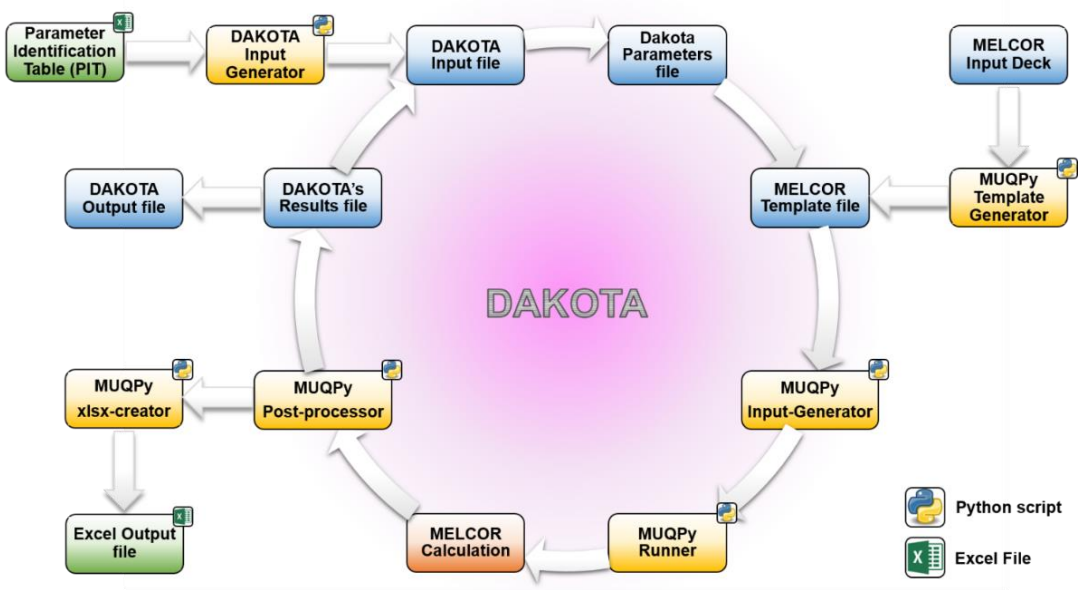

Figure 1: MELCOR-DAKOTA coupling scheme

When the UQ is conducted, it is necessary to adapt the MELCOR output to the DAKOTA format. The method employed by CIEMAT consist in define the FOMs variables with Control Functions (CFs) and write them into an External Data File (EDF) with the correct format. Then, this file is used by the DAKOTA iteration algorithm to include it in the statistical analysis. In addition, a python script is also employed to perform a parallel post-processing for the statistical analysis and also to plot all the FOMs in an Excel file.

One aspect to be accounted is that the sensitivity analysis has been performed using a relatively small sample size. This should not have any effect in parameters highly correlated with FOMs, but for robustness, it is convenient to realize a significance test. That means that the probability value (p-value) obtained for the CCs in a hypothesis test should fall below a significance level (α). The α-value is defined as $\alpha=1-\beta$, being β the confidence level desired. Therefore, for a 95% confidence $\alpha=0.05$. Since the FOM analyzed is an integral magnitude, the test is performed for values resulted at the end of the transient, that is at 20000 s.

3. MUSA-WP4: PHEBUS FPT1 Exercise

As said above, the WP4 was built to test the UQ methodologies against the PHEBUS FPT1 test. The FPT1 test involved the degradation to melting of a 1 m long fuel bundle, made of 18 irradiated fuel rods (about 24 GWd/tU), two fresh fuel rods and a silver-indium-cadmium control rod. The fuel bundle was re-irradiated in situ in order to build up a close-enough inventory in short-lived Fission Products (FPs). The degradation of the fuel was carried out by a progressive increase of the driver-core power, up to the formation of a molten pool in the lower part of the bundle. The test comprises several phases: fuel degradation-, aerosol transport, containment washing, and a chemistry-phase. However, only the first two of them were decided to be faced in WP4. More information about the PHEBUS-FPT1 test can be found in [2]. The Figures Of Merit (FOMs) are collected in Table 1.

Table 1: CIEMAT's 1st calculation Figures of Merit for the PHEBUS-FPT1 exercise

Parameter
Release of iodine from the fuel bundle [% of i.i.]
Release of cesium from the fuel bundle [% of i.i.]
Cesium retention in the circuit [% of cesium released]
Iodine airborne in the containment's atmosphere [mg]
Deposited iodine in the containment [mg]

A database has been built in MUSA WP2 (Identification and Quantification of Uncertainty Sources). Nonetheless, CIEMAT built an own database with more than 700 input MELCOR parameters, of which only those related to core degradation, FP release and aerosol dynamic processes have been included in this analysis (Table 2); a total of 56 input parameters considered. The characterization of input parameters uncertainty was done through a literature survey, as shown in the table; note that there is diversity of sources for some parameters, while no information was found for others. When several sources were found for a specific parameter, a combination was applied by selecting the minimum, maximum and expected values from the data available (note that the expected value could be the mean value or the mode). As for the probability distribution, if more than one distribution is proposed, a triangular one was used. In the case that no data were found, engineering judgement was put in place.

Table 2: CIEMAT's 1st calculation Figures of Merit for the PHEBUS-FPT1 exercise

Description	Parameter id.	Range		Exp. Val. / B.Est.	Distribution	Reference
Aerosol Resuspension Fraction [a.u.]	fractResuspend	1.00%	100.00%	100.0%	Uniform	Expert Judgment
Fission Power [W]	oprpow	89.00%	111.00%	100.0%	Uniform	[1, p. 1]

Rod spacing [m]	pitch	5.00E-03	1.50E-02	1.26E-3	Uniform	Expert Judgment (Range) / [1, p. 0] (Best Estimate value)
Laminar Nusselt Number in fully developed flow in a rod bundle with constant heat flux	C1212_2	4.36	17.81	4.36	Uniform	[2], [3]
Temperature above which conduction enhancement is employed for molten components [K]	C1250_1	2800	3200	2800	Uniform	[3], [4]
Oxidation rate constant Low Temperature (H_2O)	C1001_1_1	27.82	32.56	29.6	Uniform	[5], [6]
Oxidation rate constant High Temperature (H_2O)	C1001_3_1	79.11	93.17	87.90	Uniform	[5], [6]
Oxidation rate: Upper temperature boundary for low temperature range [K] (H_2O Oxidation)	C1001_5_1	1825.00	1875.00	1850.00	Normal	[3], [7]
Oxidation rate: Lower temperature boundary for high temperature range [K] (H_2O Oxidation)	C1001_6_1	1845.00	1895.00	1870.00	Normal	[3], [7]
Minimum oxidation temperature [K]	C1004_1	933.15	1348.16	1323.16	Normal	[3], [7]
Eutectic reaction temperature [K] (Zircaloy-Steel)	C1011_2	1200	1400	1400	Triangular	[3]
Cladding failure (FP release)	clfail	973.00	1673.00	1073.00	Lognormal	[5], [6], [8]–[10]
Fuel failure time vs. Clad temperature (TF Scale factor affecting failure time)	tfscal_23	45.0%	200.0%	100.0%	Uniform	[11]
Initial FP mass (x11 RN Classes)	rinp1_cor_	87.0%	113.0%	100.0%	Uniform	[1]
I2 in cladding gap	rinp1_clad_	0.01	0.10	0.05	Uniform	Expert Judgment
Aerosol density [kg/m^3]	rhonom	870.00	4500.00	2000.00	Triangular	[11]
Dynamic Shape Factor [a.u.]	chi	0.50	15.00	1.00	Triangular	[12] & Expert Judgment
Agglomeration Shape Factor [a.u.]	gamma	1.00	10.00	1.75	Triangular	[12] & Expert Judgment
Slip factor [a.u.]	fslip	1.01	1.51	1.26	Triangular	Expert Judgment
Condensation coefficient [a.u.]	stick	0.20	1.00	1.00	Triangular	[13]

Thermal accomodation coefficient [a.u.]	ftherm	1.00	3.00	2.25	Triangular	[14], [15].
Turbulent dissipation [m^2/s^3]	turbds	7.50E-04	3.00E-02	1.00E-03	Triangular	[14]
Gas thermal conductivity / Particle thermal conductivity [a.u.]	tkgop	6.00E-03	1.00E+00	5.00E-02	Triangular	[14]
Diffusion boundary layer thickness [m]	deldif	5.00E-06	8.00E-03	1.00E-05	Triangular	[3], [14]
ZR Specific Heat [J/kgK]	tfscal_102	80.00%	120.00%	100.0%	Uniform	Expert Judgment
ZIRCONIA Specific Heat [J/kgK]	tfscal_130	88.00%	112.00%	100.0%	Uniform	[1]
CS Specific Heat [J/kgK]	tfscal_138	80.00%	120.00%	100.0%	Uniform	Expert Judgment
SS Specific Heat [J/kgK]	tfscal_142	80.00%	120.00%	100.0%	Uniform	Expert Judgment
AGINC Specific Heat [J/kgK]	tfscal_158	80.00%	120.00%	100.0%	Uniform	Expert Judgment
Spray Coating [J/kgK]	tfscal_166	94.00%	106.00%	100.0%	Uniform	[1]
Thoria [J/kgK]	tfscal_162	95.00%	105.00%	100.0%	Uniform	[1]
ZR Thermal Conductivity [W/mK]	tfscal_103	80.00%	120.00%	100.0%	Uniform	Expert Judgment
ZIRCONIA Thermal Conductivity [W/mK]	tfscal_131	55.00%	145.00%	100.0%	Uniform	[1]
CS Thermal Conductivity [W/mK]	tfscal_139	80.00%	120.00%	100.0%	Uniform	Expert Judgment
SS Thermal Conductivity [W/mK]	tfscal_143	80.00%	120.00%	100.0%	Uniform	Expert Judgment
AGINC Thermal Conductivity [W/mK]	tfscal_159	80.00%	120.00%	100.0%	Uniform	Expert Judgment
Spray Coating [W/mK]	tfscal_167	80.00%	120.00%	100.0%	Uniform	[1]
Thoria [W/mK]	tfscal_163	65.00%	135.00%	100.0%	Uniform	[1]
ZR Density [kg/m^3]	tfscal_104	90.00%	110.00%	100.0%	Uniform	Expert Judgment
ZIRCONIA Density [kg/m^3]	tfscal_132	97.50%	102.50%	100.0%	Uniform	IPSN/DRS/SEA/PEPF, 2000)
CS Density [kg/m^3]	tfscal_140	90.00%	110.00%	100.0%	Uniform	Expert Judgment
SS Density [kg/m^3]	tfscal_144	90.00%	110.00%	100.0%	Uniform	Expert Judgment
AGINC Density [kg/m^3]	tfscal_160	90.00%	110.00%	100.0%	Uniform	Expert Judgment
Spray Coating [kg/m^3]	tfscal_168	95.00%	105.00%	100.0%	Uniform	IPSN/DRS/SEA/PEPF, 2000)
Thoria [kg/m^3]	tfscal_164	96.50%	103.50%	100.0%	Uniform	IPSN/DRS/SEA/PEPF, 2000)

The MELCOR Evaluation Model (EM) of the PHEBUS apparatus has been modeled as shown in Figure 2. The bundle is discretized into 11 axial nodes and 2 radial rings, with 2 thermal hydraulic flow channels. The circuit is divided into 18 additional nodes, this being the minimum considered necessary for an adequate calculation of deposition [2]. The containment has been modeled with a single node for the main volume and another one for the sump, taking advantage of the well-mixed conditions.

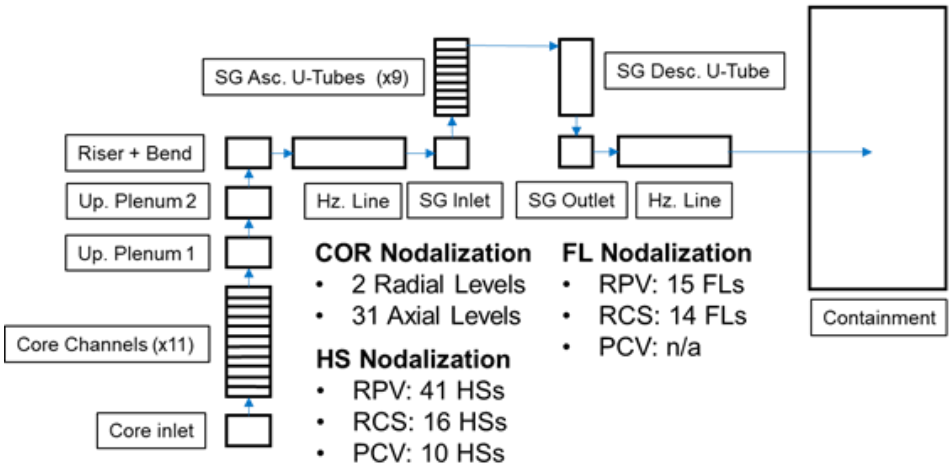

Figure 2: PHEBUS-FPT1 MELCOR nodalization

4. Results & Discussion

Results are shown in the following figures. Experimental results are not included to focus on identifying the challenges showed up by applying the above methodology to the experimental scenario. More importantly, the MELCOR evaluation model developed for the FPT1 has been thought for predictive analysis in the same way a NPP analysis would be performed. Therefore, no model calibration has been done. In addition, the experimental uncertainties, which are non-depreciable, has not been accounted. Out of the whole set of runs (93), 14 did not reach the targeted sample time (20000 s) and were considered failed. However, the analysis assumed that the entire set of calculations launched were successful; as a result, the focus has been set on trends rather than numerical results.

Cesium release from fuel is shown in Figure 3. The blue curve represents the base case result, and the red ones the upper and lower uncertainty bounds, respectively. The released mass differs in both, magnitude and timing, but what it is of interest for obtaining the tolerance interval is the quantity at the end of the transient. Therefore, the cesium released from the fuel at 20000 s ranges between 70-82 % of the initial cesium inventory in the fuel if a 95/95 criterion is applied in the analysis. Interestingly, one of the failed cases (at around 16500 seconds) shows a tendency that indicates that it would be the highest value obtained at the end of the sequence. This is of major importance when the Wilks' approach is employed, because "crash runs" might play a role, and a strategy should be figured out to deal with them.

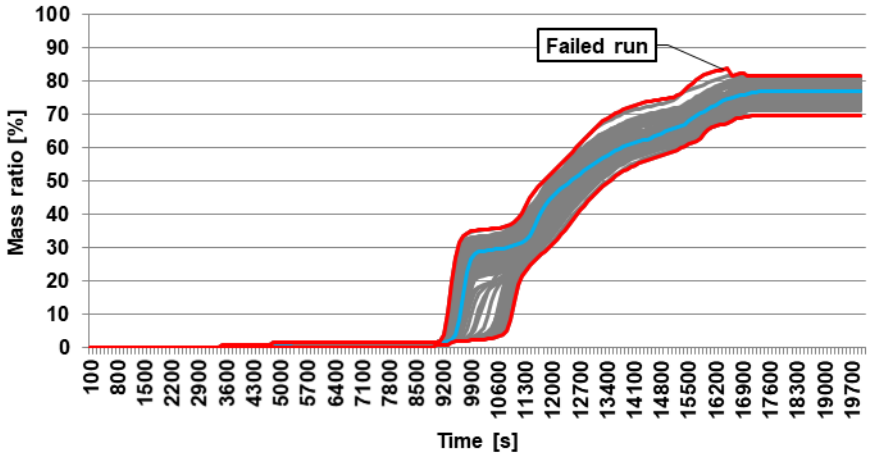

Figure 3: Released Cesium from the fuel

The Pearson correlation coefficients as a function of time can be seen in Figure 4. The first observation to make is that influence of some input parameters notably change along the transient. For instance, the red curve that reaches the value of around -0.9 corresponds to the "clfail" input variable, which represents the cladding failure temperature. If it is analyzed along with the cesium released ratio (Figure 3), it can be realized that this parameter is the dominant between 3500-9000 seconds, even though the released quantity is still small at this time. At this stage, the FP release rate is dependent on the number of failed rods, which is mainly controlled in MELCOR by the failure temperature set in the input deck. The nodalization in the COR package is also responsible for the number of failed rods along the time (the finer the mesh, the more progressive the number of leaking rods). The second period (9000-20000 s) looks dominated by the "C1212_2" and "tfscal_131" input parameters, which represents the laminar Nusselt number in fully developed flow in a rod bundle with constant heat flux, and the zirconia thermal conductivity, respectively. Both parameters are closely related with the temperature evolution in the fuel bundle, and since the released model employed (CORSOR-M) is dependent on the COR cell temperature, they both play a noticeable role during this period.

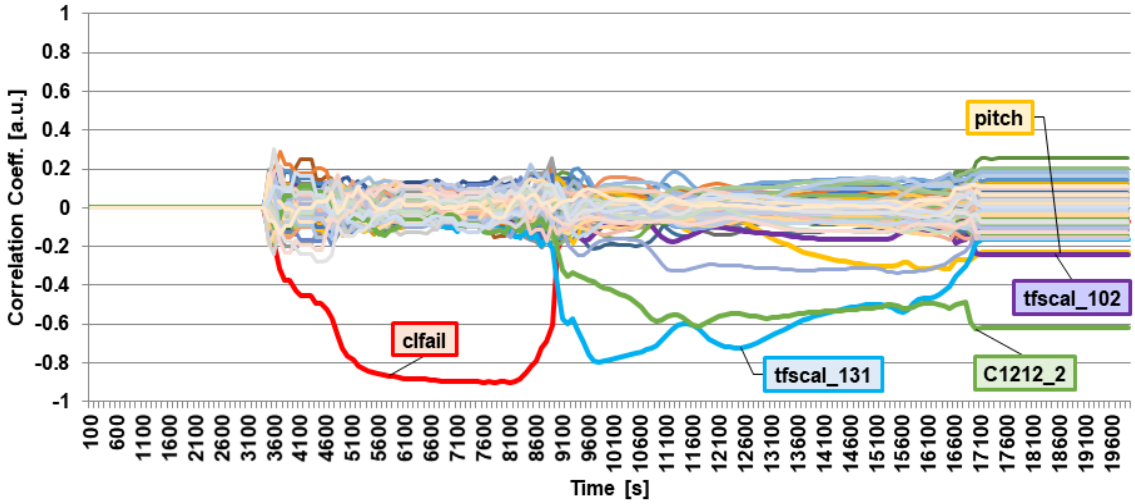

Figure 4: Pearson's correlation coefficients for the released cesium

Only the "pitch", "tfscal_102", and "C1212_2" input variables met the so called significance test. Namely, they should be the only ones considered correlated with the cesium released ratio: the pitch value (distance between fuel rods), the zirconium specific heat, and the already cited laminar Nusselt number in fully developed flow in a rod bundle with constant heat flux. Two CCs have been computed, the Pearson's and Spearman's CC (Figure 5). Both of them resulted similar in magnitude, indicating that the parameters are negatively, linearly, and monotonically descendent correlated.

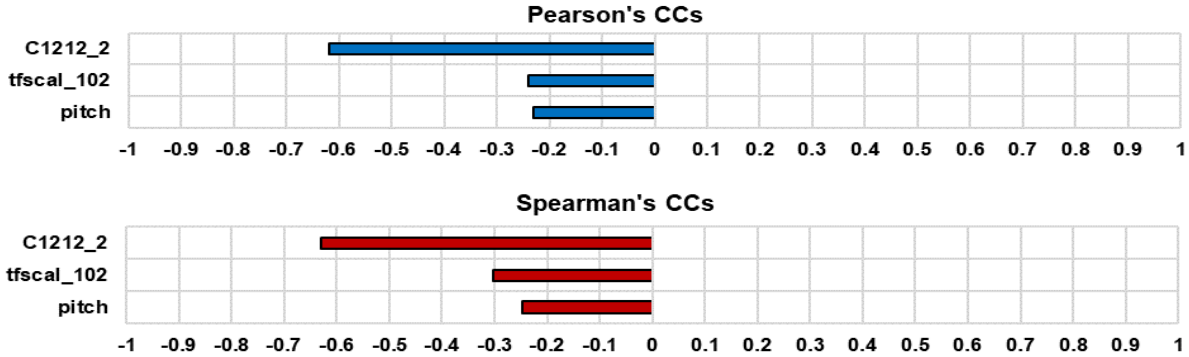

Figure 5: Released cesium correlation coefficients

Such as modeled, FP release occurs in two stages; firstly, FP located in the gap of failed fuel rods at the moment of cladding failure; secondly, FP from the pellets of the failed rods when according to temperature escalation. Another meaningful insight from the uncertainty analysis is that the release onset is rather uncertain, between 3500-9000 s, but the Cs release fraction in this period predicted in the calculation was negligible when compared to the total one. In short, uncertainty of Cs release from fuel is tightly bonded to fuel rod failure criterion, nodalization and thermal hydraulics during the first phase of an accident.

Something similar to the released cesium happens with the iodine (Figure 6), which ranges between 70-80 % of the initial iodine inventory. For this FOM, the scattering in the onset time is even more noticeable than for Cs, given that the fraction of I defined in the gap is higher.

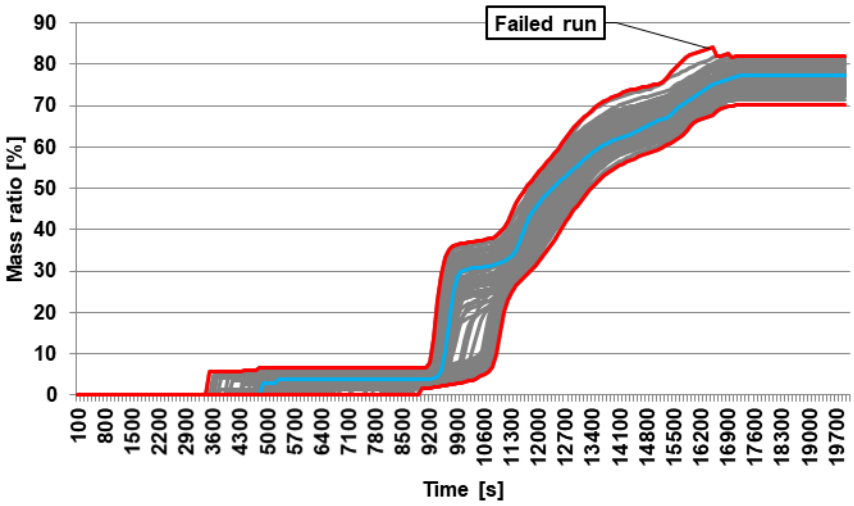

Figure 6: Released Iodine from the fuel

The correlation coefficients are shown in Figure 7. During the first stage (3500-9000 s), two parameters stand out above the rest, the “rinp1_clad_I2” and the “clfail”, referred to the proportion of iodine into the cladding gap and the cladding failure temperature, respectively. The difference with respect to cesium stems from the fact that, although both nuclides are released from the fuel according to an Arrhenius equation (i.e., temperature dependent) and get out from fuel rods at a specific clad temperature (as set in the input deck), a significant fraction of iodine inventory is initially located in the fuel rod gap. For the second release stage, the most correlated parameters resulted in the “tfscal_139” and “C1212.2”, being the “tfscal_139” referred to the carbon steel thermal conductivity.

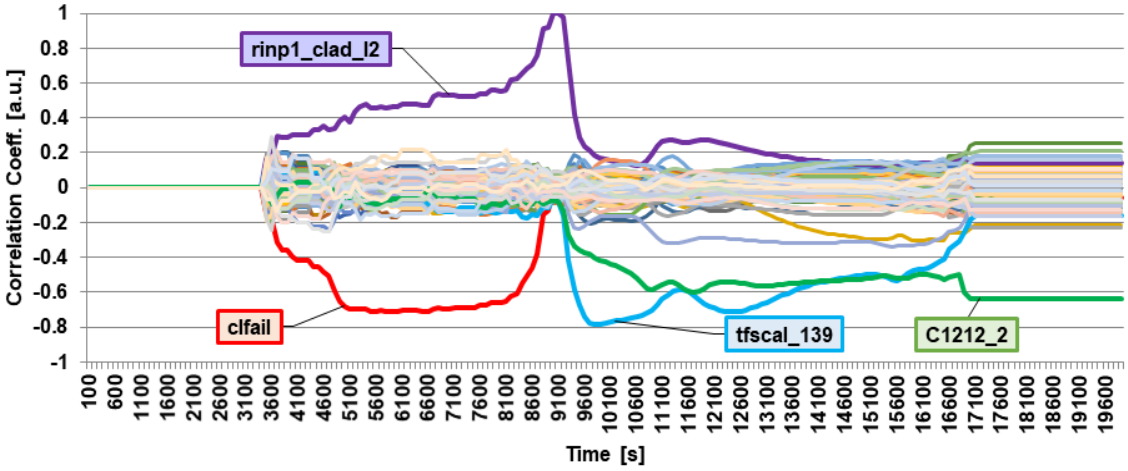

Figure 7: Pearson's CCs for the released iodine

The significance test is also performed for values at the end of the sequence (20000 s). It is not surprising that three of the four parameter CCs with statistical significance are the same than that for the cesium release (see Figure 8). Both, the cesium and iodine, are volatile FPs, thus it is expected to be governed by the same release equation. In MELCOR, the FP release is only estimated for the cesium class. For obtaining the release rate for all the other classes, a proportional multiplier is applied to the cesium release rate. The last remaining parameter included in Figure 8, the "tfscal_139", is positive and weak (~22%). Both its absolute contribution and its positive sign may be hardly supported on physical grounds, so that it might be considered a casualty due to the small sample employed in the sensitivity analysis.

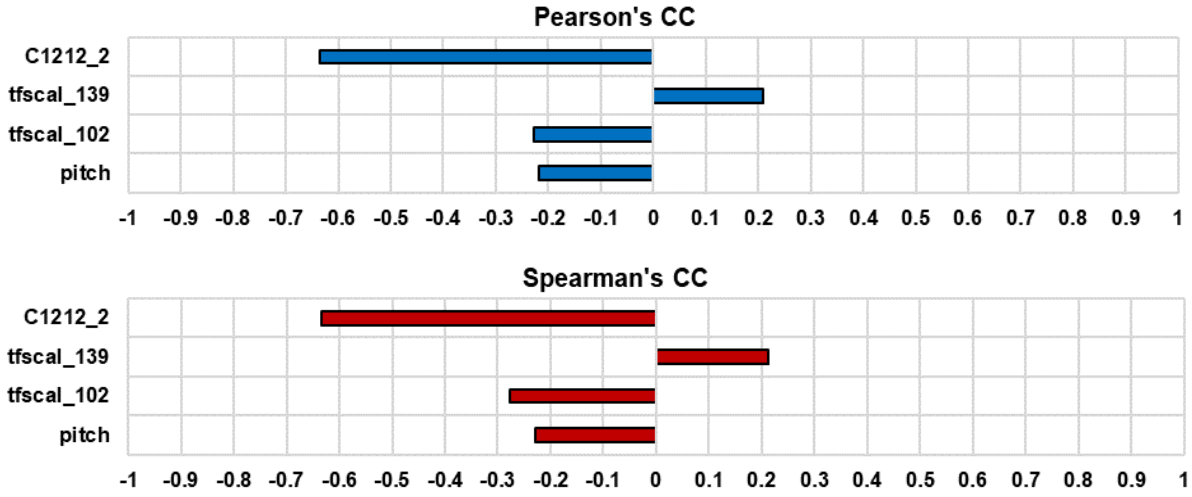

Figure 8: Released iodine correlation coefficients

The cesium deposits in the circuit in relation to that released from fuel are shown in Figure 9 as a function of time. However, the study interest is focused on the final cesium deposits (at the end of the transient), and it resulted in a range between 6-63 %.

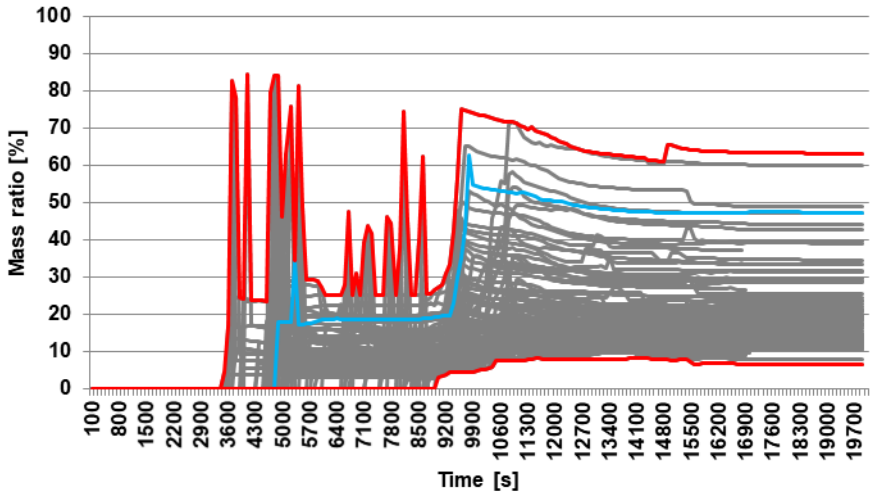

Figure 9: Cesium deposited in the circuit

This phenomenon is characterized to produce peaks between roughly 3000 and 9000 s, which are related with the cladding failure rate according to the clad failure criterion discussed above. Anyway, the quantitative impact of these peaks is negligible when the amount released is noted (see Figure 3 and Figure 6). Then, the deposition is mainly governed by the aerosol dynamics, and this can be confirmed looking at the correlation coefficients computed (see Figure 10). Only 2 out of the 86 input parameters included in the analysis could be considered correlated after the significant test, and both of them, "ftherm" and "chi", are parameters related with the calculation of the aerosol transport phenomena. The parameter "ftherm" represent the thermal accommodation coefficient and "chi" the aerosol dynamic shape factor. "Both the "chi" Spearman's CC (~99%) and the Pearson's CC (~76%) show very high values. This finding is consistent with the effect of inertial removal mechanisms on the overall deposition process. On the other hand, "ftherm" is also correlated for both CCs, although to a noticeable less extent.

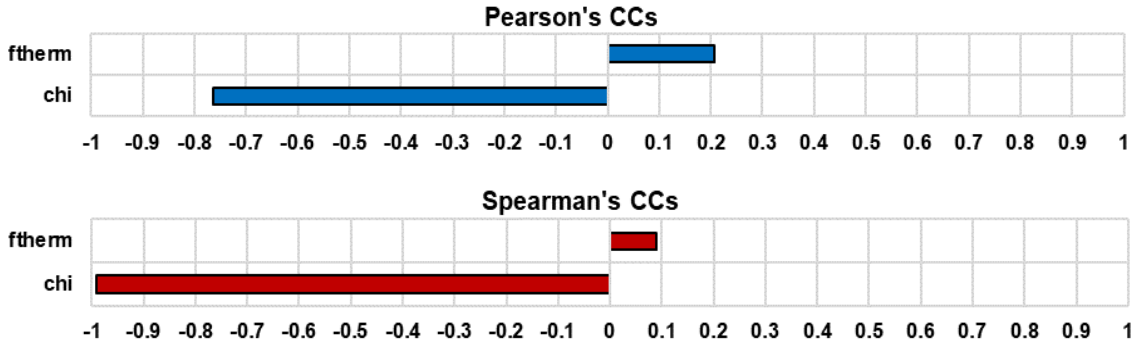

Figure 10: Cesium retained in circuit correlation coefficients

The mass of particulate iodine in containment is shown in Figure 11. The magnitude at the end of the transient ranges between 177-477 g, increasing the results dispersion along the transient.

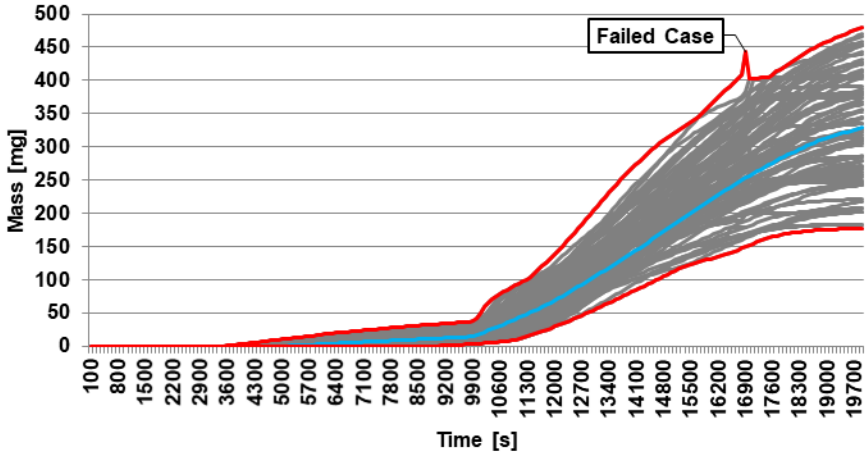

Figure 11: Iodine aerosol mass in containment

The Pearson's CCs are shown in Figure 12. As observed, uncertainties are heavily correlated with those of the release, which highlights the fact that transport to containment is, to a good extent, transparent in "uncertainty" terms ("clfail", "rinp1_cor_I2", "tfscal_131"). Then, once in the containment, uncertainties affecting other parameters governing aerosol dynamics, like "chi" or "gamma", also become visible. In other words, this FOM inherits uncertainties occurring in previous processes affecting the transport to and in containment.

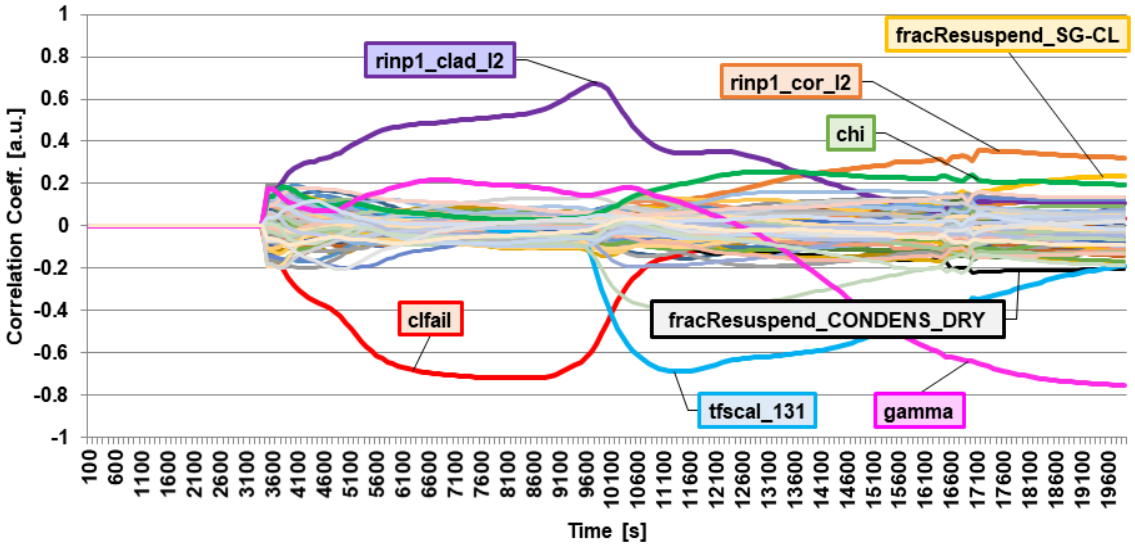

Figure 12: Pearson's CCs for the iodine aerosol mass in containment

From all the parameters analyzed, those whose CC present a statistical significance at the end of the transient (t=20000 s) are the "fractResuspend_SG-CL", "fractResuspend_CONDENS_DRY", "rinp1_cor_I2", "gamma", and "turbds", which represent the resuspension fraction of aerosols into the steam generator tube, the resuspension fraction of aerosols over the containment condenser (dry part), the initial inventory of iodine within the fuel, the agglomeration shape factor and the turbulent dissipation respectively. Their resultant CCs for both, Pearson's and Spearman's, are shown in Figure 13. As can be seen, the parameters correlated are those involved in the quantity of iodine available in the system and those related to the transport of aerosols from the fuel bundle to the containment, being the most influencing the gamma factor, with a negative CC of almost -0.8. This is again physically consistent: the bigger the iodine particles are (i.e., higher average agglomeration rate), the less the probability of remaining airborne in containment.

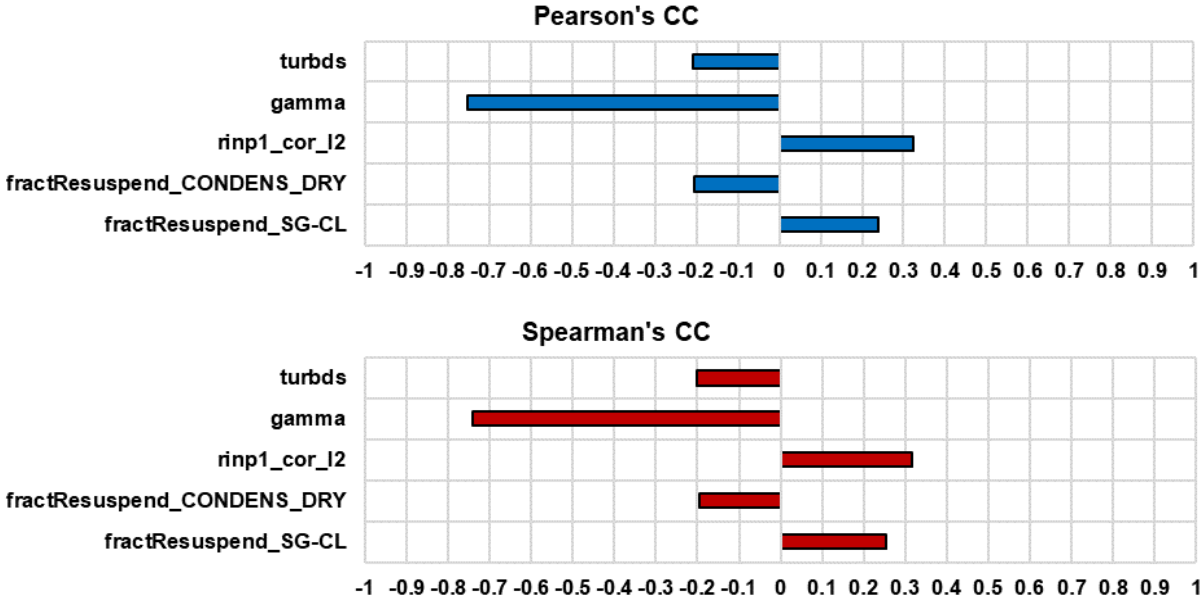

Figure 13: Total iodine aerosol in containment correlation coefficients

The last FOM analyzed is the iodine deposited in containment, which is shown in Figure 14. The total mass deposited at the end of the transient ranges from 311 to 800 mg. However, this interval "does not tell the entire story" as several cases crashed and some of them might have become bounding cases. The uncertainty in the deposited iodine in containment increases while the FPs are released into the system and transported through it to the containment; the profile closely follows the one in Fig. 11 (in-containment airborne iodine). The main factors governing uncertainties till 9000 s are the iodine inventory available, and those parameters noted in the analysis of release rate computation (Figure 15).

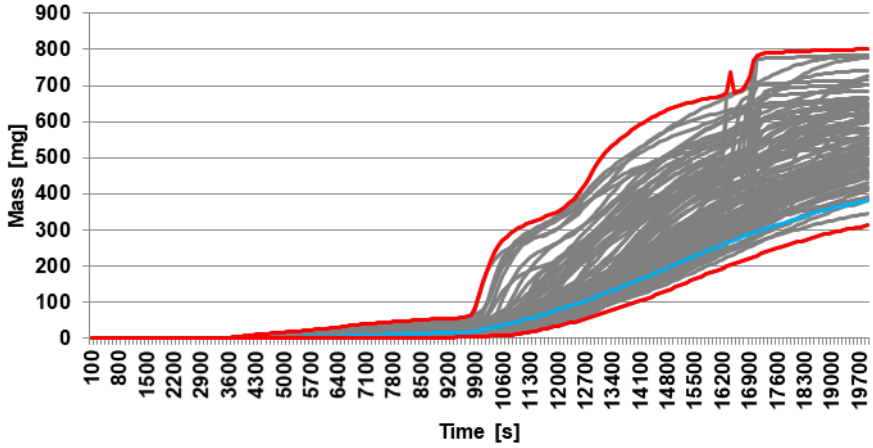

Figure 14: Iodine deposited in containment

The CCs with statistical significance at the end of the transient are shown in Figure 16. As expected, "rin1_cor_I2", "tfscal_131", "chi" and "gamma" are the parameters that can be said with a 95% confident that are correlated with the quantity of iodine deposited into the containment. The "chi" parameter corresponds to dynamic shape factor involved in the computation of the aerosol dynamics, particularly in sedimentation (dominating removal mechanism in containment). The other has already been discussed above.

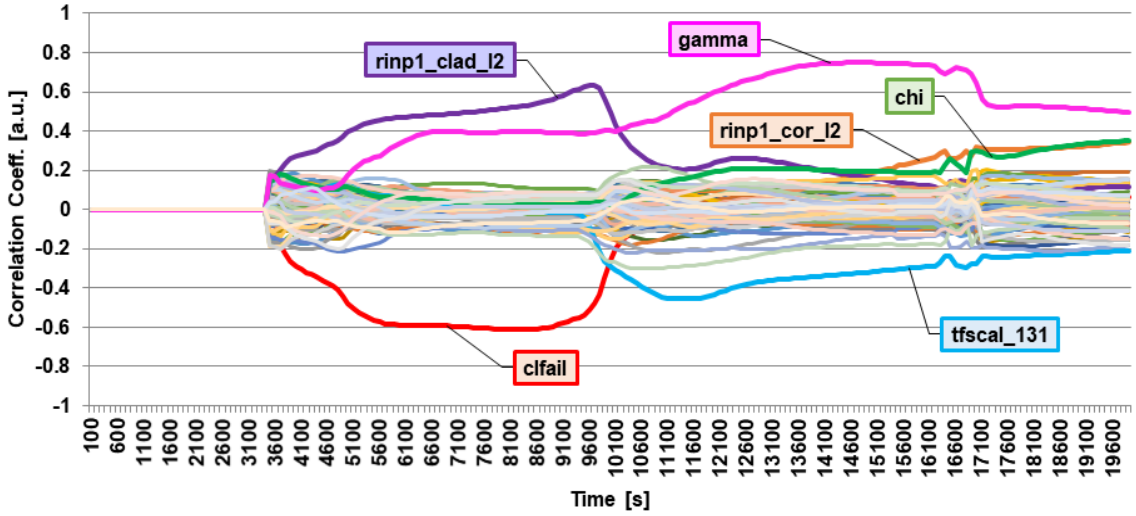

Figure 15: Pearson's CCs for the deposited iodine mass in containment

Both CCs, Pearson's and Spearman's, are almost identical indicating that the correlation is highly linear and increasing monotonically, except for the "tfscal_131" which is negative. The agglomeration shape factor

"gamma" resulted the most influencing (~50%), followed by the dynamic and iodine inventory in the fuel (~35%).

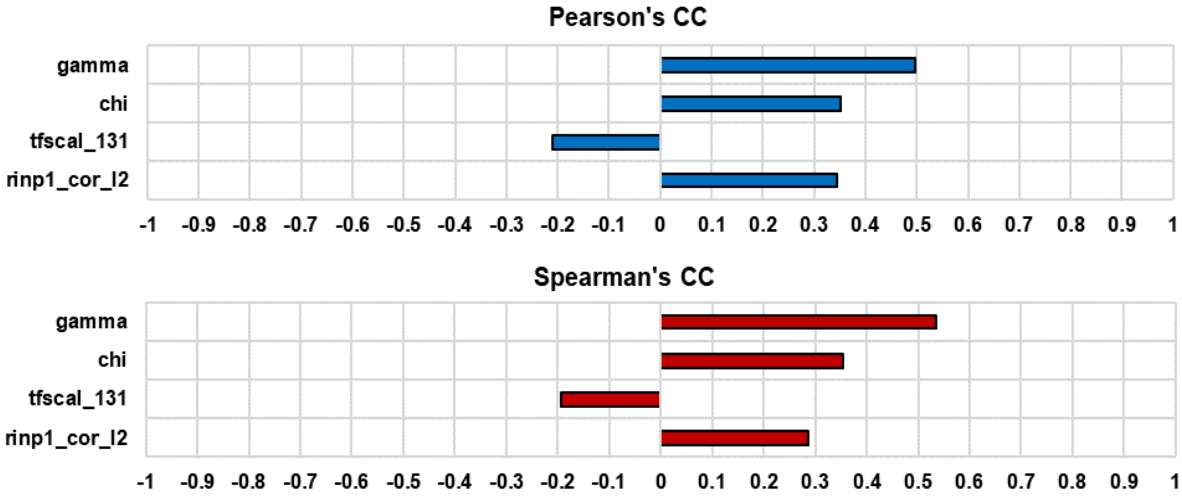

Figure 16: Iodine deposited in containment correlation coefficient

5. Final Remarks

Under the framework of the EU-MUSA project, focused on the application of the BEPU approach to severe accident analyses, the CIEMAT's methodology for uncertainty quantification has been tested against the scenario setup in the FPT1 experiment of the PHEBUS program. Two aspects have been given the utmost interest: on a practical side, the MELCOR-DAKOTA coupling through python scripts; on a conceptual one, how to manage the calculation database to gain deep and sound insights into the scenario predictability. Given the scope of MUSA and the FPT1 setup, FOMs concerning fission products release from fuel and transported through the facility were chosen.

From the work done, some generic observations have been settled:

- The extreme and intrinsic complexity of severe accident scenarios. The number of phenomena involved in severe accidents is huge and entails different disciplines, from thermal-hydraulics to aerosol physics, chemistry, structural mechanics and many others. This and the close interlink of many of them make particularly complicated to conduct a thorough identification and characterization of input deck parameters whose uncertainties should be propagated through the calculation. In the case of FPT1, with the specific focus already mentioned, more than 700 parameters have been identified in MELCOR 2.2; in the root of this large set is the close link of source term phenomena and thermal-hydraulics.
- Even when the number of parameters are drastically reduced (56) to make the trial applications more manageable, the adoption of the Wilk's method to limit the number of runs needed (93 for a 95% probability and 95% confidence) turns code crashes into a non-negligible matter. Replacing them by alternate ones might lead to an ill-coverage of the sampling domain, which would handicap the robustness of the calculation database. The more acceptable option seems to conduct a deep study of the crashes to identify the reasons underneath and make them work. Some authors (NEA/CSNI, 2017) suggest increasing the Wilks' order to allow discarding higher FOM's values, but this implicitly assume that the failed cases are those corresponding to the higher FOM's magnitudes.
- Sensitivity analysis might be a powerful tool to exploit the calculation database, but further work is necessary to find a suitable way of carrying it out. On one side, the regression techniques used in this work have been limited to the traditional Pearson and Spearman coefficients and further data analysis techniques should be explored to find out their potential. On the other, it is highly recommended to

conduct the so called significance test to identify parameters with a relevant role in the FOM's uncertainties; however, it should be expected that other variables than those accomplishing the significance test might be also correlated, as the size of the calculations database is limited. This said, by crossing the statistical information with the physical understanding of the scenario provides sound arguments supporting the identification through the significance test.

Additionally, some lessons from this exercise might be also drawn concerning Source Term FOMs:

- In-containment FOMs inherit uncertainties involved in fission product release and transport. Namely, those input parameters visibly influencing release and transport do also affect containment variables. What is interesting is that some of those variables, particularly those related to the time onset, are structural variables which setting are closely related to thermal-hydraulics.
- Uncertainties affecting in-containment FOMs grow with time, as expected, and at the end-of-transient their scatter does not exceed a factor of 2.0 with respect the baseline calculation. What might be of interest, though, is that uncertainties in fission product release onset might extend in a range of hours. This sort of observations might be of high relevance for practical implementation of accident management actions, if confirmed.
- Particles shape uncertainties do directly affect their transport and deposition mechanisms and, consequently, do have an observable impact in related source term FOMs other than release from the fuel. If confirmed when modeling NPP severe accidents, this might be a worth-to-investigate issue.

The natural steps of this work are: its extension to a larger set of input deck uncertain parameters and noticing the major discrepancies, if any, with the study here presented; application of the CIEMAT's approach to NPP severe accident analysis, both in reactor (MUSA/WP5) and in SFP (MUSA/WP6).

REFERENCES

1. IPSN/DRS/SEA/PEPF, «PHEBUS FPT1 Final Report», Cadarache, France, 2000.
2. T. L. Bergman y F. P. Incropera, Eds., *Fundamentals of heat and mass transfer*, 7th ed. Hoboken, NJ: Wiley, 2011.
3. Sandia National Laboratories, *MELCOR 2.2 Code Manuals*. Albuquerque, New Mexico: Sandia National Laboratories, 2019.
4. Sandia National Laboratories, «State-of-the-Art Reactor Consequence Analyses Project. MELCOR Best Modeling Practices», Sandia National Laboratories, Albuquerque, New Mexico, NUREG NUREG/CR-7008, 2010.
5. F. Sanchez-Saez, A. I. Sánchez, J. F. Villanueva, S. Carlos, y S. Martorell, «Uncertainty analysis of a large break loss of coolant accident in a pressurized water reactor using non-parametric methods», *Reliability Engineering & System Safety*, vol. 174, pp. 19-28, 2018, doi: 10.1016/j.ress.2018.02.005.
6. E. Zugazagoitia *et al.*, «Uncertainty and sensitivity analysis of a PWR LOCA sequence using parametric and non-parametric methods», *Reliability Engineering & System Safety*, vol. 193, p. 106607, 2020, doi: 10.1016/j.ress.2019.106607.
7. V. F. Urbanic y T. R. Heidrick, «HIGH-TEMPERATURE OXIDATION OF ZlRCALOY-2 AND ZIRCALOY-4 IN STEAM», *Journal of Nuclear Materials*, vol. 75, pp. 251-261, 1978.
8. NRC, «Cladding Swelling and Rupture Models for LOCA Analysis», NRC, NUREG-0630, 1980. [En línea]. Disponible en: https://www.nrc.gov/docs/ML0534/ML053490337.pdf
9. D. Y. Oh, J. Lee, Y. S. Bang, y C. Yang, «Uncertainty Evaluation considering Burnup Effect during LBLOCA», p. 12, 2017.

10. G. Schanz, S. Hagen, P. Hofmann, G. Schumacher, y L. Sepold, «Information on the evolution of severe LWR fuel element damage obtained in the CORA program», *Journal of Nuclear Materials*, vol. 188, pp. 131-145, 1992, doi: https://doi.org/10.1016/0022-3115(92)90462-T.

11. US NRC, «SOARCA Uncertainty Analysis of the Unmitigated Long-Term Station Blackout of the Peach Bottom Atomic Power Station», US NRC, NUREG/CR-7155, 2016. Accedido: 30 de enero de 2020. [En línea]. Disponible en: https://www.nrc.gov/docs/ML1318/ML13189A145.pdf

12. S. Y. Park y K. I. Ahn, «Uncertainty Analysis of the Fission Product Behaviors during Severe Accidents for a Typical PWR», *Progress in Nuclear Science and Technology*, vol. 1, n.º 0, Art. n.º 0, 2011, doi: 10.15669/pnst.1.448.

13. M. Mozurkewich, «Aerosol Growth and the Condensation Coefficient for Water: A Review», *Aerosol Science and Technology*, vol. 5, n.º 2, Art. n.º 2, 1986, doi: 10.1080/02786828608959089.

14. J. C. Helton, R. L. Iman, J. D. Johnson, y C. D. Leigh, «Uncertainty and Sensitivity Analysis of a Model for Multicomponent Aerosol Dynamics», *Nuclear Technology*, vol. 73, n.º 3, Art. n.º 3, 1986, doi: 10.13182/NT86-A16075.

15. L. Talbot, R. K. Cheng, R. W. Schefer, y D. R. Willis, «Thermophoresis of particles in a heated boundary layer», *J. Fluid Mech.*, vol. 101, n.º 4, Art. n.º 4, 1980, doi: 10.1017/S0022112080001905.